

## Downflow Etching of Si Using a Microwave- Excited Discharge Plasma of Ar/CF<sub>4</sub> Mixtures

Tsuji, Masaharu  
Institute of Advanced Material Study Kyushu University

Okano, Shinji  
Department of Applied Science for Electronics and Materials Graduate School of Engineering  
Sciences Kyushu University

Tanaka, Atsushi  
Department of Applied Science for Electronics and Materials Graduate School of Engineering  
Sciences Kyushu University

Tanoue, Takeshi  
Department of Applied Science for Electronics and Materials Graduate School of Engineering  
Sciences Kyushu University

他

<https://doi.org/10.15017/7930>

---

出版情報 : 九州大学機能物質科学研究所報告. 15 (1), pp.11-17, 2001. Institute of Advanced  
Material Study Kyushu University

バージョン :

権利関係 :

# Downflow Etching of Si Using a Microwave-Excited Discharge Plasma of Ar/CF<sub>4</sub> Mixtures

Masaharu TSUJI, Shinji OKANO\*, Atsushi TANAKA\*,  
Takeshi TANOUE\*, and Takeshi TSUJI

Downflow etching of Si was studied using a microwave-excited discharge plasma of Ar/CF<sub>4</sub> mixtures under conditions that would produce less plasma-damage than that in our previous experiments [M. Tsuji *et al.*, *Jpn. J. Appl. Phys.*, **38**, 6470 (1999)]. A long distance between the center of discharge and the substrate (20 cm) was used in order to reduce plasma-damage of the Si surface. The maximum etching rate was about 700 Å/min at a microwave power of 80 W, an Ar flow rate of 2500 sccm, and a CF<sub>4</sub> flow rate of 300 sccm. A thin C<sub>m</sub>F<sub>n</sub> polymer was deposited along the edges of etched region at high CF<sub>4</sub> flow rates above about 100 sccm. It was characterized using a XPS.

## Introduction

Since plasma etching is generally carried out by setting a material to be etched directly in an etching discharge plasma, high-plasma-damage due to accelerated particles often occurs.<sup>1-3)</sup> In the downflow etching process, plasma is generated at an upstream location away from the substrate and the etchants generated in the plasma are transported by the gas flow into the etching chamber. Therefore, the downflow etching process is a highly selective low-plasma-damage process.<sup>3-5)</sup> Recently, we have studied the chemical dry etching of Si using a discharge-flow method, which is one of the downflow etching processes.<sup>6,7)</sup> F atoms were generated by a microwave discharge of various Ar/CF<sub>4</sub> mixtures at an upstream location away from the Si substrate. They were used as etchants of Si substrates at room temperature. By adding Ar to CF<sub>4</sub>, a stable microwave discharge could be maintained at a low output power (< 200 W). The variation in etching rate was measured as a function of the microwave power, the Ar or CF<sub>4</sub> flow rate, and the distance between the center of discharge and the substrate, in order to determine the optimum conditions. The maximum etching rate was about 700 Å/min at a microwave power of 80 W, an Ar flow rate of 3000 sccm, a CF<sub>4</sub> flow rate of 70 sccm, and a distance between the center of discharge and the substrate of 10 cm. A surface analysis using a scanning Auger indicated that a thin C<sub>m</sub>F<sub>n</sub> polymer was deposited along the edges of the etched region at high CF<sub>4</sub> flow rates of 80-100 sccm.

When the Si surface, etched under the above

conditions, was observed using a scanning electron microscope (SEM), significant surface damage was found, as will be shown in the first paragraph of Results and Discussion. Therefore, in the present study, chemical dry etching of Si using a discharge-flow method was reinvestigated under low-damage conditions. The extent of surface damage after etching was examined using a SEM. A thin C<sub>m</sub>F<sub>n</sub> polymer was deposited on the etching edge at high CF<sub>4</sub> flow rates. Its structure was characterized using a X-ray photoelectron spectrometer (XPS).

## Experimental

The discharge-flow chemical dry etching chamber used in this study is similar to that reported previously.<sup>6,7)</sup> In brief, it consists of a stainless-steel main flow tube (internal diameter 250 mm), a quartz discharge tube (internal diameter 11 mm), and a substrate holder. A Teflon sheet was inserted into the quartz discharge tube. The apparatus was continuously evacuated using a 5 m<sup>3</sup>/min booster pump backed by a 1.5 m<sup>3</sup>/min rotary oil pump. Ar and CF<sub>4</sub> gases were kept at constant flow rate and mixtures of various ratios were fed into the microwave discharge operated at an output power of 80 W. The pressure in the etching chamber was measured using a Pyrani gauge calibrated against a capacitance manometer.

A Si(100) substrate (10 × 10 mm<sup>2</sup>) was placed 20 cm downstream from the center of the microwave discharge. The distance between the exit opening of the quartz discharge tube and the substrate was kept at a constant value of 4 cm in this study. A thin stainless-steel mask

---

Received February 5, 2001

Dedicated to Professor Yukio Nishimura on the occasion of his retirement

\* Department of Applied Science for Electronics and Materials, Graduate School of Engineering Sciences, Kyushu University.

(thickness = 0.2 mm) with a hole (diameter = 3.75 mm) and a Teflon sheet (thickness = 0.3 mm) were used to cover the substrate. The etching profiles were measured using an Alpha Step 200. Thin films deposited on the Si surface were analyzed using a XPS (Shimadzu ESCA-1000) and an ULVAC PHI scanning Auger nanoprobe system (SAM-680) equipped with SEM.

Optical emission spectra of the Ar/CF<sub>4</sub> discharge were measured in the 200-830 nm region using a Spex 1250M monochromator equipped with a cooled Hamamatsu Photonics R376 photomultiplier. Analog signals from the photomultiplier were converted to digital ones using an AD converter, and they were stored and analyzed in a microcomputer. The relative sensitivities of the monochromator and the photomultiplier were calibrated using standard D<sub>2</sub> and halogen lamps.

### Results and Discussion

Figure 1(a) shows a SEM photograph of the Si surface etched under the optimum conditions used in the previous study.<sup>7)</sup> The distance between the center of discharge and the substrate was kept at 10 cm. Many holes due to significant surface damage by direct exposure to the plasma are observed. Similar surface damage was observed, when Si was etched by discharge products of pure Ar gas. Therefore, ion bombardment by Ar<sup>+</sup> may be the main reason for the surface damage observed using the Ar/CF<sub>4</sub> mixture at 10 cm. In order to reduce such plasma damage, the distance between the center of discharge and the substrate was set at the longer distance of 20 cm, which was the longest distance possible in our present apparatus. When a SEM photograph of Si surface was measured, it could be seen that the surface damage was greatly reduced, as shown in Fig. 1(b). Therefore, we have reexamined optimum etching conditions when using the long distance of 20 cm by varying other experimental parameters such as Ar and CF<sub>4</sub> flow rates. When Si was etched at the long distance of 20 cm, the etching rate decreased by about 40% in comparison with that at 10 cm. This is mainly due to a decrease in the concentration of etchant F atoms by more collisions with the quartz surface of the discharge tube. In order to reduce such a loss of [F] in a discharge flow, a thin Teflon sheet (thickness = 0.3 mm and length = 10 cm) was inserted into the quartz tube between the discharge and the exit opening of the discharge tube. As a result, the etching rate increased by 40%, so that the loss of [F] at a longer distance was recovered. All experiments reported in this study were carried out using the Teflon sheet.

Figure 2 shows the variation in the etch depth as a function of the etching time. The etch depth increases slowly at a short etching time below 5 min probably due to a slow etching rate of natural oxide (SiO<sub>2</sub>; thickness about 100 Å) covered on the Si surface. It increases

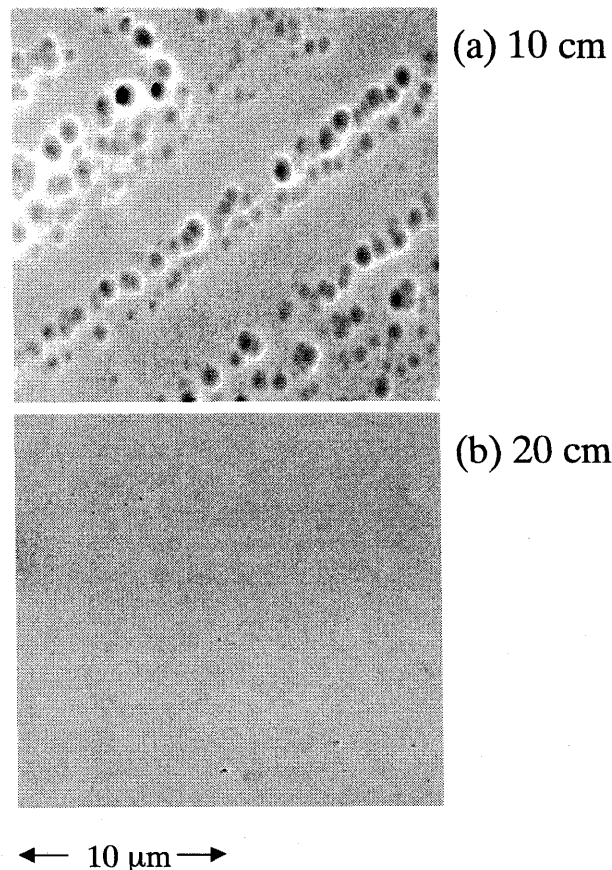


Fig. 1. A SEM photograph of Si surface etched at a microwave power of 80 W, Ar and CF<sub>4</sub> flow rates of 2500 and 150 sccm, respectively, a total pressure of 0.28 Torr, and a distance between the center of discharge and the Si substrate of (a) 10 cm and (b) 20 cm.

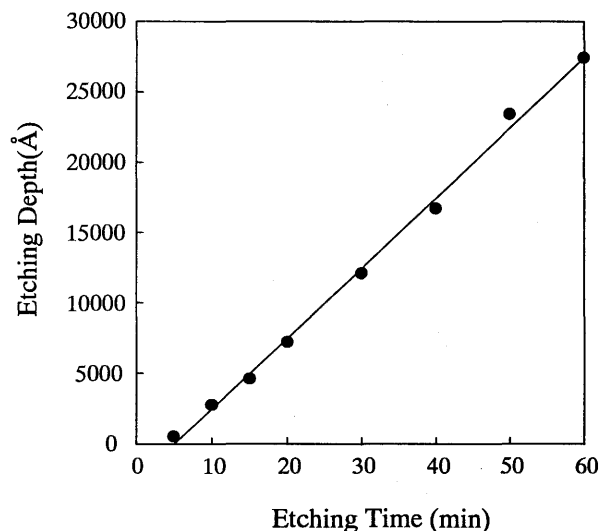


Fig. 2. Variation in the etch depth as a function of the etching time at a microwave power of 80 W, Ar and CF<sub>4</sub> flow rates of 2500 and 150 sccm, respectively, a total pressure of 0.28 Torr, and a distance between the center of discharge and the Si substrate of 20 cm.

linearly with increasing etching time from 5 to 60 min. This indicates that the etching rate of Si is independent of the etching time once a native SiO<sub>2</sub> film on the Si surface has been removed. From the slope of Fig. 2, the etching rate was determined to be 300 Å/min under these conditions.

Figure 3 shows the variation in the etching rate as a function of the Ar flow rate. For comparison, the dependence of [F] on the Ar flow rate obtained using CH(A-X) emission due to the Ar(<sup>3</sup>P<sub>0,2</sub>)/CH<sub>3</sub> reaction<sup>8)</sup> is also shown. The etching rate peaks at an Ar flow rate of about 2500 sccm. The dependence of the etching rate on the Ar flow rate is similar to that of [F] on the Ar flow rate. This implies that the dominant etchant is F atom and the dependence of etching rate on the Ar flow rate reflects the variation in [F] for the Ar flow rate. It is known that the active species generated by a microwave discharge of pure Ar gas are metastable Ar(<sup>3</sup>P<sub>0,2</sub>) atoms, ground-state Ar(<sup>2</sup>P<sub>1/2,3/2</sub>) ions, and metastable Ar<sup>+</sup> ions.<sup>9-12)</sup> The available energies of Ar(<sup>3</sup>P<sub>0</sub>) and Ar(<sup>3</sup>P<sub>2</sub>) atoms are 11.75 and 11.55 eV, and those of Ar(<sup>2</sup>P<sub>1/2</sub>) and Ar(<sup>2</sup>P<sub>3/2</sub>) ions are 15.92 and 15.76 eV, respectively. There exist many metastable argon ions with available excitation energies of 16.41-20.27 eV for Ar<sup>+</sup> → Ar<sup>+</sup> excitation transfer and those of 17.87-22.19 eV for Ar<sup>+</sup> → Ar<sup>+</sup> charge transfer.<sup>9-11)</sup> The dependence of the relative concentrations of the above active species of Ar on the pressure of the Ar buffer gas was monitored by observing the N<sub>2</sub>(C<sup>3</sup>Π<sub>u</sub>-B<sup>3</sup>Π<sub>g</sub>), ArKr<sup>+</sup>(C<sub>1</sub> 3/2-A<sub>1</sub> 3/2), and CH(A<sup>2</sup>Δ-X<sup>2</sup>Π) emissions resulting from the following reference reactions at a constant reagent gas pressure.<sup>12-14)</sup>

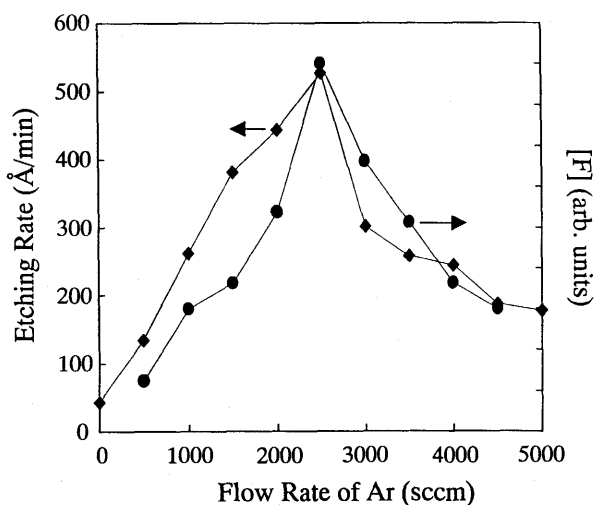
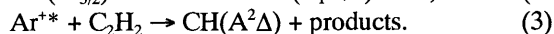
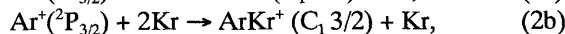
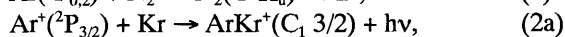
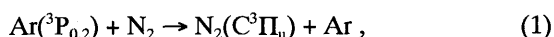


Fig. 3. Dependence of the etching rate and [F] on the Ar flow rate. The other experimental parameters were the same as those for Fig. 2.

The results obtained were the same as those reported in previous experiments and obtained at 10 cm.<sup>7)</sup> [Ar(<sup>3</sup>P<sub>0,2</sub>)] exhibited a sharp peak at a low Ar flow rate of about 2000 sccm, while [Ar<sup>+</sup>] and [Ar<sup>++</sup>] increased more slowly with increasing Ar flow rate and exhibited a peak at higher Ar flow rates of 4000 and 4500 sccm, respectively. The variation in the relative concentrations of each Ar active species with Ar pressure in pure Ar gas may not be the same as that in the Ar/CF<sub>4</sub> mixtures used for the Si etching. However, it is reasonable to assume that at first, Ar atoms are excited or ionized by a microwave discharge and then F atoms are generated by the reactions of active Ar species with CF<sub>4</sub> at Ar flow rates of 500-2000 sccm. The etching rates at low Ar flow rates of 500-2000 sccm are about 25-85% of the maximum etching rate at 2500 sccm. Since the dominant Ar active species in this range is Ar(<sup>3</sup>P<sub>0,2</sub>), Ar(<sup>3</sup>P<sub>0,2</sub>) will be significant for the generation of F atoms from the microwave discharge of the Ar/CF<sub>4</sub> mixture at Ar flow rates below about 2000 sccm. Although [Ar(<sup>3</sup>P<sub>0,2</sub>)] decreases significantly at Ar flow rates above 2500 sccm, such a great decrease in the etching rate is not observed at high Ar flow rates of 2500-5000 sccm, where the dominant active species of Ar are Ar<sup>+</sup> and Ar<sup>++</sup>. Therefore, these ionic active species are expected to be significant for the generation of F atoms at high Ar flow rates above 2500 sccm.

Figure 4 shows the variation in the etching rate as a function of CF<sub>4</sub> flow rate at two Ar flow rates of 2500 and 3000 sccm along with our previous data at 10 cm in the CF<sub>4</sub> flow rate range of 0-100 sccm and variation in [F] for CF<sub>4</sub> flow rate.<sup>6,7)</sup> At a short distance of 10 cm, the deposition of thin C<sub>m</sub>F<sub>n</sub> polymers was found on the etching edge at CF<sub>4</sub> flow rates above 80 sccm. It is

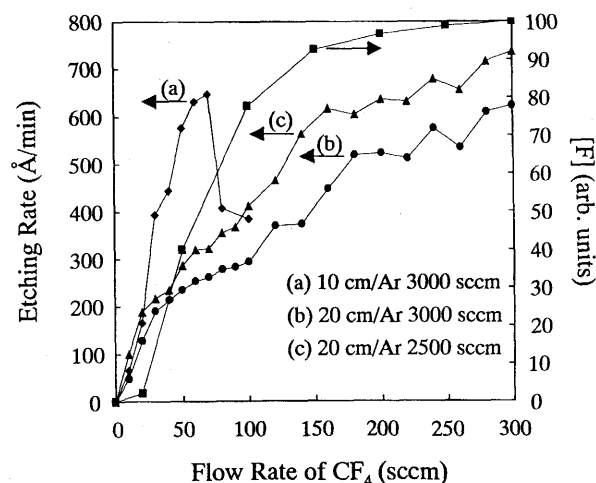


Fig. 4. Dependence of the etching rate on the CF<sub>4</sub> flow rate. The other experimental parameters were the same as those for Fig. 2. For comparison, dependence of the etching rate on the CF<sub>4</sub> flow rate at a distance between the center of discharge and the Si substrate of 10 cm is also shown.

known that  $CF_n$  ( $n=0-3$ ) are precursors of  $C_mF_n$  polymers, which are often deposited during plasma etching when using fluorocarbons.<sup>2,3)</sup> Among them,  $CF_2$  radical is believed to be the most important precursor.<sup>15-17)</sup> The deposition of thin  $C_mF_n$  polymers prevents the Si surface from being etched. Oehrlein and Williams<sup>18)</sup> have found that the Si etching rate is controlled by the  $C_mF_n$  film and that it is directly proportional to the inverse of the  $C_mF_n$  film thickness for fluorocarbon films thicker than about 10 Å. Thus, the decrease in the etching rate in the 80-100 sccm region will be due to the fact that thick  $C_mF_n$  films are deposited at 10 cm during the etching process. In the present study at 20 cm, such a decrease in the etching rate is not found and the etching rate increases with increasing the  $CF_4$  flow rate to 300 sccm. The etching rates tend to level off above about 150 sccm in both Ar flow rates of 2500 and 3000 sccm. It should be noted that the dependence of the etching rate on the  $CF_4$  flow rate is similar to that of [F] on the  $CF_4$  flow rate. This led us to conclude that the dependence of the etching rate on the  $CF_4$  flow rate reflects the variation in [F] for the  $CF_4$  flow rate at a long distance of 20 cm. Although deposition of  $C_mF_n$  films were observed at  $CF_4$  flow rates above about 100 sccm (see below), no decrease in the etching rate was found. This suggests that thick  $C_mF_n$  films were not deposited at 20 cm.

Figure 5 shows the dependence of the etching rate on the total pressure in the etching chamber at three different  $CF_4$  flow rates. The total pressure in the etching chamber was varied by closing or opening a variable gate valve between the etching chamber and the booster pump. The etching rates increase from 0.3 to 0.6-0.7 Torr and slightly decrease at pressures above that. Figure 5 demonstrates that the etching rate can be enhanced by a factor of 2-3 by elevating the total

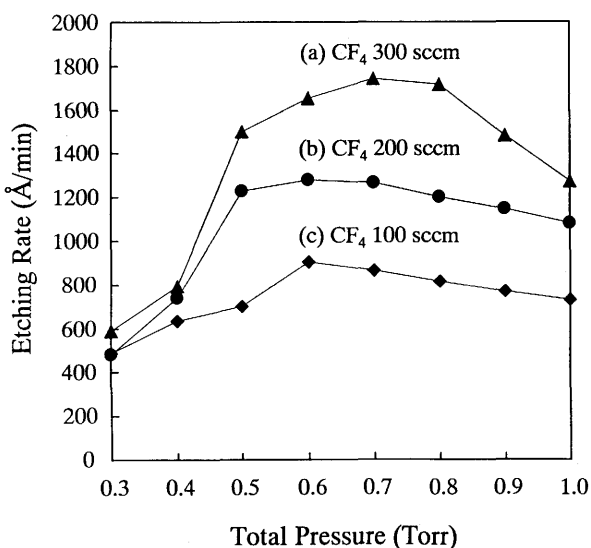
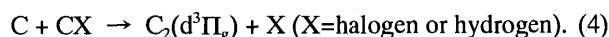


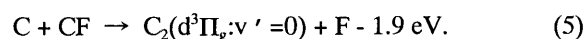
Fig. 5. Dependence of etching rate on the total pressure in the etching chamber. The other experimental parameters were the same as those for Fig. 2.

pressure. We have measured a linear flow velocity of the Ar flow by measuring a time of flight (TOF) of electrons or  $Ar^+$ . The TOF spectra were obtained by pulsing an electrostatic potential applied to a charged particle collector and measuring the arrival time of charged particles at a Langmuir probe placed 12.5 cm downstream from the charged particle collector. It was found that the linear flow velocity of the Ar flow was about 20,000  $cm\ s^{-1}$  at 0.3 Torr and decreased with increasing the total pressure by reducing the pumping rate. Our results indicate that the flow rate of [F] has a maximum at a total pressure of 0.6-0.7 Torr. One reason for the increase in the [F] below 0.6-0.7 Torr is an increase in the residence time of Ar/ $CF_4$  stream in the discharge region due to a decrease in the flow velocity. The slight decrease at higher pressures is probably due to a loss of F by secondary collisions.

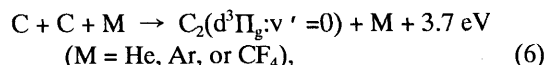
Excited species, generated in the discharge region, were identified by observing emission spectra in the discharge region. When pure  $CF_4$  was used, discharge could not be maintained at a low microwave power of 80 W. However, at a high microwave power of  $\geq 150$  W, a stable discharge could be maintained. Figure 6(a) shows a typical emission spectrum in the 200-600 nm region resulting from the discharge of pure  $CF_4$  at a microwave power of 150 W. The  $CF(A^2\Sigma^+-X^2\Sigma^+, B^2\Sigma^+-X^2\Sigma^+)$ ,  $CF_2(A^2\Sigma^+-X^2\Sigma^+)$ , the  $C_2$  Swan system ( $d^3\Pi_g-a^3\Pi_u$ ), and the CN Violet system ( $B^2\Sigma^+-X^2\Sigma^+$ ) are observed. A similar  $C_2$  band has been found by Arnold *et al.*<sup>19)</sup> in a discharge of halogenated methanes of the form  $CH_{2-n}X_{2+n}$  ( $X=Cl, Br, I$ ). They predicted that the  $C_2(d-a)$  band predominantly arises from the following reaction:



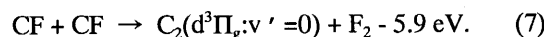
For  $CF_4$ , the corresponding process (4) is endoergic:



Therefore, the above process can be excluded from possible excitation mechanism of  $C_2(d)$ . The most probable excitation mechanism of  $C_2(d)$  is the following three-body recombination reaction:



because the following two-body process is highly endoergic:



The CN(B-X) emission was strongly enhanced by the addition of a small amount of NO 10 cm downstream from the center of the discharge. This must arise from the four center  $C_2/NO$  reaction,<sup>20-23)</sup> where NO results from a small amount of residual  $N_2$  and  $O_2$  in the

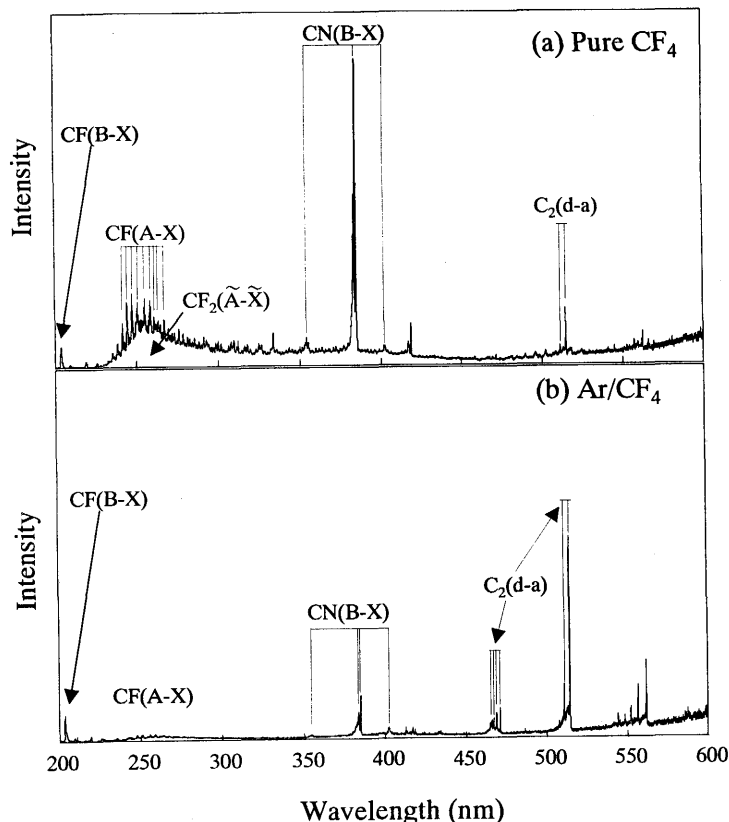


Fig. 6. Typical emission spectra resulting from discharge of (a) pure  $\text{CF}_4$  and (b)  $\text{Ar}/\text{CF}_4$  mixture.

discharge tube:



When Ar was added, a stable microwave discharge could be maintained at a low microwave power. Figure 6(b) shows a typical emission spectrum obtained from a mixture of  $\text{Ar}/\text{CF}_4$  at a microwave power of 50 W. It should be noted that  $\text{CF}(\text{B-X})/\text{CF}_2(\text{A-X})$  intensity ratio becomes large,  $\text{C}_2(\text{d-a})$  emission becomes strong, and the  $\text{CN}(\text{B-X})$  emission becomes weak by the Ar addition. These results suggest that a higher extent of decomposition occurs by the addition of Ar into  $\text{CF}_4$ . Therefore, an advantage of the addition of Ar is an enhancement of decomposition of  $\text{CF}_4$ , which will lead to a higher concentration of etchant F atoms.

Figure 7 shows the dependence of the emission intensities of  $\text{CF}(\text{A-X})$ ,  $\text{CF}(\text{B-X})$ ,  $\text{CF}_2(\text{A-X})$ ,  $\text{C}_2(\text{d-a})$ , and  $\text{CN}(\text{B-X})$  on the  $\text{CF}_4$  flow rate. All of the emission systems have a maximum at the lowest  $\text{CF}_4$  flow rate of 1 sccm, and decreases from that to 10 sccm. Above the  $\text{CF}_4$  flow rate of 10 sccm, the emission intensities of  $\text{CF}(\text{A-X})$  and  $\text{CF}_2(\text{A-X})$  increase, while those of  $\text{CF}(\text{B-X})$ ,  $\text{C}_2(\text{d-a})$ , and  $\text{CN}(\text{B-X})$  decrease with an increase in the  $\text{CF}_4$  flow rate. The dependence of the emission intensities of  $\text{CF}(\text{A-X})$  and  $\text{CF}_2(\text{A-X})$  on the  $\text{CF}_4$  flow rate above 10 sccm is similar to that of the etching rate and  $[\text{F}]$ , as shown in Fig. 4. On the basis of these findings, it could be demonstrated that the variation in

$[\text{CF}(\text{A})]$  and  $[\text{CF}_2(\text{A})]$  for the  $\text{CF}_4$  flow rate is similar to that of  $[\text{F}]$  above 10 sccm.

Auger spectra were measured in order to obtain information on the deposition of the  $\text{C}_m\text{F}_n$  polymer. Although no evidence of a deposition of  $\text{C}_m\text{F}_n$  polymers was found at  $\text{CF}_4$  flow rates below 100 sccm, a

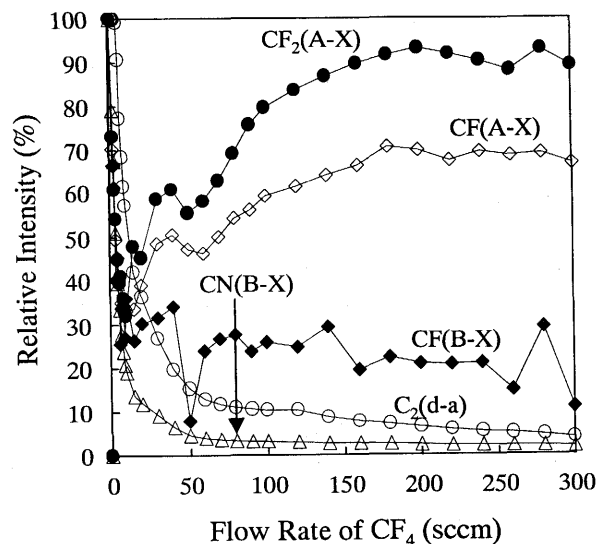


Fig. 7. Dependence of emission intensities of  $\text{CF}(\text{A-X})$ ,  $\text{CF}(\text{B-X})$ ,  $\text{CF}_2(\text{A-X})$ ,  $\text{C}_2(\text{d-a})$ , and  $\text{CN}(\text{B-X})$  on the  $\text{CF}_4$  flow rate. The other experimental parameters were the same as those for Fig. 2.

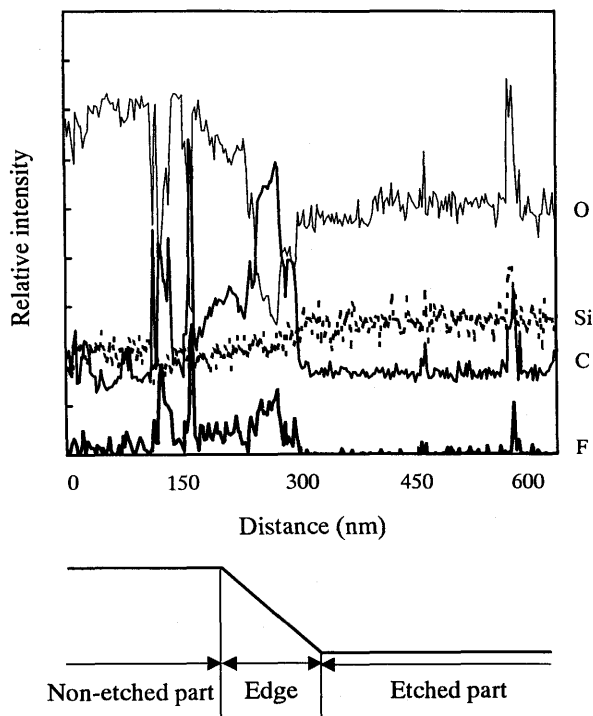


Fig. 8. A typical Auger line spectrum of Si substrate. Dependence of intensities of Auger peaks of F, Si, O, and C atoms on the distance on the substrate. The other experimental parameters were the same as those for Fig. 2 except for a lower  $\text{CF}_4$  flow rate of 100 sccm.

deposition of  $\text{C}_m\text{F}_n$  polymers was found above that. Figure 8 shows a typical Auger line spectrum. The Auger peaks in the etched and non-etched parts consist of O, Si, and C, where O peak is due to contamination. It should be noted that, along the edge of the etched region, a F peak appears and the C peak becomes strong, while the O peak becomes weak. On the basis of these findings, it was concluded that a  $\text{C}_m\text{F}_n$  polymer is deposited along the edge. The deposition of  $\text{C}_m\text{F}_n$  polymer gives direct evidence that the  $\text{CF}_2$  radical, which is a precursor of the  $\text{C}_m\text{F}_n$  polymer, is involved at high  $\text{CF}_4$  flow rates.

$\text{C}_m\text{F}_n$  polymers deposited along the edge were characterized using a XPS. Figures 9(b)-9(d) show XPS spectra of Si surface etched at  $\text{CF}_4$  flow rates of 100, 150, and 200 sccm, respectively. For comparison, XPS spectrum of a non-etched Si surface is also shown in Fig. 9(a). In Fig. 9(a), a strong peak of C-C due to contamination is found. In Fig. 9(b), the C-C peak becomes weak, and three peaks, which can be ascribed to  $\text{CF}_3$ ,  $\text{CF}_2$ , and CF, are observed. With increasing the  $\text{CF}_4$  flow rate from 100 to 200 sccm, the relative intensities of the C peak to those of  $\text{CF}_x$  increases, as shown in Figs. 9(b)-9(d). This implies that the C/F ratio in the  $\text{C}_m\text{F}_n$  polymers increases with increasing  $\text{CF}_4$  flow rate. When the XPS spectra of Si surface were measured at  $\text{CF}_4$  flow rates of 250 and 300 sccm, the

spectra obtained were similar to that found at a  $\text{CF}_4$  flow rate of 200 sccm. On the basis of this finding, the C/F ratio can be said to be unchanged in the high  $\text{CF}_4$  flow rate range of 200-300 sccm.

### Concluding Remarks

The chemical dry etching of a Si substrate placed downstream from a microwave discharge of Ar/ $\text{CF}_4$  mixtures has been reinvestigated at low-plasma-damage-

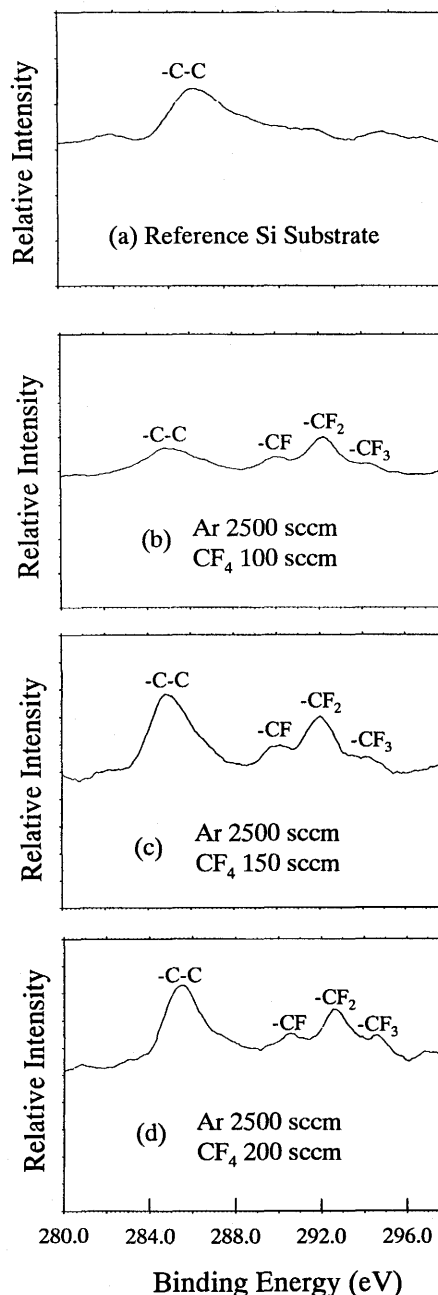


Fig. 9. XPS spectra of Si surface: Si substrate (a) without etching and (b)-(d) etched at  $\text{CF}_4$  flow rates of 100, 150, and 200 sccm, respectively. The other experimental parameters were the same as those for Fig. 2.

conditions by inserting a Teflon sheet into the discharge tube. The dependence of the etching rate on the experimental parameters was determined by measuring the etch depth. The maximum etching rate was about 700 Å/min at a microwave power of 80 W, an Ar flow of 2500 sccm, a CF<sub>4</sub> flow of 300 sccm, a total pressure of 0.28 Torr, and a distance between the center of discharge and the substrate of 20 cm. This value is the same as that obtained in our previous experiment at a short distance of 10 cm.<sup>7)</sup> The SEM and XPS observations of etched surfaces indicate that C<sub>m</sub>F<sub>n</sub> polymers are deposited along the edges of the etched region at CF<sub>4</sub> flow rates above about 100 sccm.

### References

1. "Glow Discharge Processes: Sputtering and Plasma Etching," ed. by B. N. Chapman, Wiley, New York (1980).
2. "Photon and Plasma Processings," ed. by K. Akashi, S. Hattori, and O. Matsumoto, Nikkan Kougyo Shinbunsha, Tokyo (1986), p. 211.
3. "Semiconductor Etching Technology," ed. by T. Tokuyama, Sangyo Tosho, Tokyo (1992).
4. Y. Horiike and M. Shibagaki, in "Semiconductor Silicon 1977," Vol. 77-2, ed. by H. R. Huff and E. Sirtle, Electrochem. Soc. Symp. Princeton (1977), p. 1071.
5. B. E. E. Kastenmeier, P. J. Matsuo, J. J. Beulens, and G. S. Oehrlein, *J. Vac. Sci. & Technol.*, **A 14**, 2802 (1996).
6. M. Tsuji and Y. Nishimura, *Jpn. J. Appl. Phys.*, **36**, 6922 (1997).
7. M. Tsuji, S. Okano, A. Tanaka, and Y. Nishimura, *Jpn. J. Appl. Phys.*, **38**, 6470 (1999).
8. M. Tsuji, H. Kouno, Y. Nishimura, H. Obase, and K. Kasatani, *J. Chem. Phys.*, **95**, 7313 (1991).
9. M. Tsuji, in "Techniques of Chemistry," Vol. 20, ed. by J. M. Farrar and W. H. Saunders, Jr., Wiley, New York (1988), p. 489.
10. T. Matsuo, N. Kobayashi, and Y. Kaneko, *J. Phys. Soc. Jpn.*, **50**, 3482 (1981).
11. T. Matsuo, N. Kobayashi, and Y. Kaneko, *J. Phys. Soc. Jpn.*, **51**, 1558 (1982).
12. T. D. Nguyen and N. Sadeghi, *Chem. Phys.*, **79**, 41 (1983).
13. M. Tsuji, M. Tanaka, and Y. Nishimura, *Chem. Phys. Lett.*, **256**, 623 (1996).
14. K. Suzuki and K. Kuchitsu, *J. Photochem.*, **10**, 401 (1979).
15. R. D'Agostino, F. Cramarossa, V. Colaprico, and R. d'Ettole, *J. Appl. Phys.*, **54**, 1284 (1983).
16. T. Goto and M. Mori, *Jpn. J. Appl. Phys.*, **32**, 4850 (1993).
17. G. Cunge and J. P. Booth, *J. Appl. Phys.*, **85**, 3952 (1999).
18. G. S. Oehrlein and H. L. Williams, *J. Appl. Phys.*, **62**, 662 (1987).
19. S. J. Arnold, G. H. Kimbell, and D. R. Snelling, *Can. J. Chem.*, **53**, 2419 (1975).
20. H. F. Krause, *J. Chem. Phys.*, **70**, 3871 (1979).
21. H. Reisler, M. Mangir, and C. Wittig, *J. Chem. Phys.*, **71**, 2109 (1979).
22. J. B. Lurle and M. A. El-Sayed, *J. Phys. Chem.*, **84**, 3348 (1980).
23. N. Nishiyama, H. Sekiya, M. Tsuji, and Y. Nishimura, *Rep. Inst. Adv. Mater. Study, Kyushu Univ.*, **1**, 35 (1987).

---

We thank Professor Nobuyuki Imaishi for the use of the Alpha Step and XPS spectrometer. This work was partially supported by the Mitsubishi Foundation and a Grant-in-Aid for Scientific Research (No. 09440201) from the Ministry of Education, Science, Sports, and Culture.